Polarization-modulation setup for ultrafast infrared anisotropy experiments to study liquid dynamics

Tros, M.; Woutersen, S.

Polarization-modulation setup for ultrafast infrared anisotropy experiments to study liquid dynamics

Martijn Tros and Sander Woutersen*

Van 't Hoff Institute for Molecular Sciences, University of Amsterdam, Science Park 904, 1098 XH Amsterdam, The Netherlands
*Corresponding author: s.woutersen@uva.nl

An infrared pump-probe setup using rapid polarization modulation has been developed to perform time-resolved vibrational anisotropy measurements. A photo-elastic modulator is used as a rapidly switchable half-wave plate, enabling the measurement of transient absorptions for parallel and perpendicular polarizations of the pump and probe pulses on a shot-to-shot basis. In this way, infrared intensity fluctuations are nearly completely canceled, significantly enhancing the accuracy of the transient-anisotropy measurement. The method is tested on the OD-stretch vibration of HDO in H_2O, for which the signal-to-noise ratio is found to be 4 times better than with conventional methods. © 2015 Optical Society of America

OCIS codes: (300.6340) Spectroscopy, infrared; (300.6500) Spectroscopy, time-resolved; (320.7150) Ultrafast spectroscopy.
http://dx.doi.org/10.1364/OL.40.002607

The advent of light sources generating high-intensity, sub-picosecond infrared (IR) pulses has made it possible to observe the orientational motion of molecules in liquids in a direct manner. In particular, hydrogen-bonded liquids such as water are currently intensively investigated in experiments that track the random orientational motion of liquid molecules in real time. In these experiments, an intense, linearly polarized IR-pump pulse resonantly excites part of the molecules to the first vibrationally excited ($v = 1$) state of a specific intramolecular (typically C–H, O–H or N–H-stretching) mode. The distribution of excited bonds is initially anisotropic, but eventually becomes isotropic due to random orientational motion of the molecules or hopping of the excitation from one molecule to another. By measuring the decay of the anisotropy, the random motion is tracked in real time. This is done by measuring the pump-induced anisotropic IR-absorption change ΔA with a delayed probe pulse that is polarized either parallel ($\parallel$) or perpendicularly ($\perp$) to the pump pulse. From these two quantities, one constructs the anisotropy

$$R(\tau) = \frac{\Delta A_{\parallel}(\tau) - \Delta A_{\perp}(\tau)}{\Delta A_{\parallel}(\tau) + 2\Delta A_{\perp}(\tau)} \tag{1}$$

as a function of the time τ between the pump and probe pulses. It can be shown that $R(\tau)$ is proportional to the second-order correlation function of the random orientational motion of the vibrationally excited bonds [1]. Vibrational anisotropy decays were first measured in bromoform and water in organic solvents [2,3], and since then in many other liquids, such as alcohols [4–7], water and aqueous solutions [8–20], and water in confinement [18] and at surfaces [21].

A major problem in measuring $R(\tau)$ for molecular vibrations in liquids is the short lifetime of the $v = 1$ state (often on the order of a ps), as a consequence of which $\Delta A_{\parallel}$ and $\Delta A_{\perp}$ decrease rapidly with increasing τ, making it generally difficult to determine $R(\tau)$ accurately for τ larger than a few ps. Currently, this problem is solved by

successively measuring $\Delta A_{\parallel}$ and $\Delta A_{\perp}$ using a polarizer placed in the probe beam [9,17], and averaging many successive parallel and perpendicular measurements to improve the signal-to-noise ratio. That this method is not very efficient can be understood as follows. Fluctuations in the intensity and beam pointing of the IR pulses cause identical percentual fluctuations in $\Delta A_{\parallel}$ and $\Delta A_{\perp}$. Hence, if $\Delta A_{\parallel}$ and $\Delta A_{\perp}$ were measured simultaneously, the IR fluctuations would pose no problem for accurately measuring $R(\tau)$, since the numerator and the denominator in Eq. (1) would fluctuate in the same manner, so that the fluctuations would be visible in $\Delta A(\tau)$, but would cancel out in R. However, $\Delta A_{\parallel}$ and $\Delta A_{\perp}$ can only be measured successively; and so the IR fluctuations will only cancel out in R if they occur more slowly than the time between the successive measurements of $\Delta A_{\parallel}$ and $\Delta A_{\perp}$. This, however, is generally not the case. To determine the time scale of the fluctuations of the most commonly used type of ultrafast IR source (an optical parametric amplifier pumped by an amplified Ti:sapphire laser), we measured its intensity autocorrelation function; see Fig. 1. We find a characteristic time scale of about 200 ms for the IR fluctuations, and similar time scales have been observed in other labs [22]. The contributions of shot noise, the noise in our detection electronics, and bit noise are negligible compared to the IR-intensity fluctuations. We find that the power spectrum of the fluctuations scales with frequency approximately as $1/f^2$. The characteristic time scale of 200 ms of the IR fluctuations implies that the existing methods to measure $R(\tau)$, in which successive $\Delta A_{\parallel}$ and $\Delta A_{\perp}$ measurements are carried out by rotating a polarizer or half-wave plate (which takes much longer than 200 ms), are intrinsically inefficient, often necessitating extremely long averaging times.

Here, we present a method that circumvents this problem by measuring $\Delta A_{\parallel}$ and $\Delta A_{\perp}$ alternately on a shot-to-shot basis. In this way, the IR fluctuations cancel out nearly completely in the anisotropy, resulting in a better signal-to-noise ratio of the anisotropy.
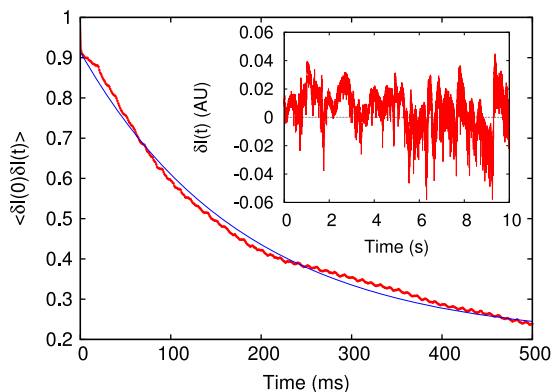
Fig. 1.   Autocorrelation function of the fluctuations in intensity of the IR pulses (thick red curve). An exponential fit (thin blue curve) gives a decay time of 180 ms. The inset shows the fluctuations with respect to the average intensity during the first 10 s of the measurement.

Figure 2 shows a schematic of the setup. Using a two-stage β-barium borate-based optical parametric amplifier and difference-frequency generation of signal and idler, we generate 4-μm wavelength mid-IR pulses [19]. The pulses have an energy of 20 μJ, 100 fs duration, a center frequency of 2500 cm^{-1}, and a ~200 cm^{-1} bandwidth. A small fraction of the IR beam is split off to obtain probe and reference pulses, and the major part (~90%) is used as pump pulse. The probe beam is led through a photo-elastic modulator (PEM; Hinds instruments, II/ZS50 ZnSe optical head, PEM-100 controller), to which the laser is synchronized in such a way that the probe polarization changes every other shot. The PEM optical axis is at 45° with respect to the incoming probe polarization. In this way, the PEM acts as a half-wave plate switched on and off at 4 times the PEM's frequency of 50 kHz. In a similar manner as reported previously [23–26], the laser system is electronically synchronized with the PEM by doubling the 100-kHz (2f) output frequency of the PEM and dividing this signal by 199, resulting in a 1005-Hz signal. This 1005-Hz signal is used to trigger the regenerative amplifier, ensuring that the probe pulses pass the PEM when it acts as a half-wave plate or leaves the polarization unchanged, thereby rendering the polarization of every other probe pulse parallel and perpendicular to that of the pump pulse.

The pump beam is optically chopped at a quarter of the laser repetition rate, and we measure alternately four probe shots where the sample is excited and four shots where the pump is blocked. The probe pulse is alternately parallel and perpendicularly polarized with respect to the pump pulse. The pump and probe beams are focused and overlapped in the sample by means of an $f = 100$ mm off-axis (30°) parabolic mirror (focal diameter 250 μm). We optimize the angle of the PEM optical axis and the relative phase of the PEM and laser by temporarily inserting a polarizer at the position of the sample and simultaneously minimizing the alternating probe transmissions when the polarizer is set parallel and perpendicular to the pump polarization. Directly behind the sample, a $\lambda/4$ plate changes the probe polarization from linear to circular to eliminate the polarization dependence of the spectrograph transmittance [27]. The probe and reference beams are then focused into a spectrograph (Oriel MS260i), where both beams are spectrally dispersed and imaged onto a 2×32 HgCdTe detector array. The digitized detector signals are processed together with the electronic PEM and chopper signals to keep track of the polarization and pump-on/off status of each observed probe pulse. The successive parallel and perpendicularly pumped transient-absorption signals $\Delta A_\parallel$ and $\Delta A_\perp$ are calculated from the recorded transmittance of the parallel or perpendicular probe pulse in the presence ($T_{\parallel,\perp}$) and absence (T_0) of the pump pulse as $\Delta A_{\parallel,\perp} = -\log(T_{\parallel,\perp}/T_0)$. From these values, we obtain the anisotropy using Eq. (1). The investigated sample was a 6% HDO in H_2O solution kept between two 1-mm-thick CaF$_2$ windows separated by a 25-μm teflon spacer.

Figure 3(b) shows the parallel and perpendicular transient signals at a probe frequency of 2508 cm^{-1} obtained
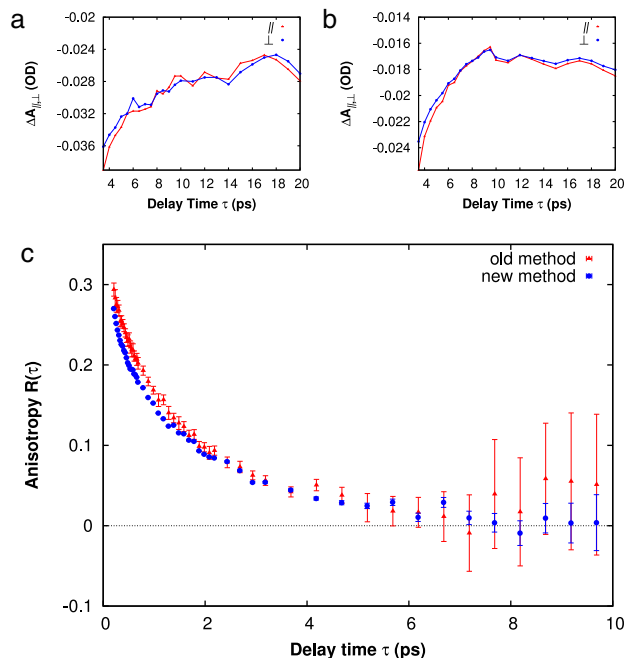
Fig. 3.   (a), (b) Single delay scans showing transient absorptions $\Delta A_\parallel$ and $\Delta A_\perp$ recorded by the conventional (a) and new (b) setup. (c) From the $\Delta A_{\parallel,\perp}$ signals obtained by averaging several scans, the anisotropies and their respective errors can be calculated for the old and new setups. The two datasets were obtained from the same total number of shots.
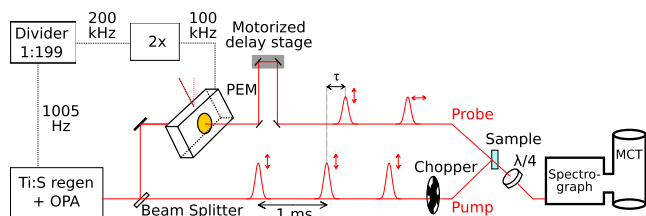

Fig. 2.   Schematic of the new polarization-resolved pump-probe infrared setup. The PEM optical axis is at 45° with respect to the polarization of the incoming probe pulse, and the polarization (two-sided arrows) is alternately parallel and perpendicular to that of the pump pulse. The pump-probe delay τ is controlled by the motorized delay stage.

with the new setup. The fluctuations in the parallel and perpendicular signals are clearly correlated. On the other hand, in Fig. 3(a), no correlation is seen for the parallel and perpendicular signals obtained with the conventional pump-probe setup [28] in which many consecutive shots are averaged to determine $\Delta A_\parallel$ and $\Delta A_\perp$ [in Figs. 3(a) and 3(b), the signals at each delay point are the averages of the same total number of shots]. An excited-state lifetime of 1.9 ps is obtained from the isotropic signal of both measurements, in agreement with previous work [17]. In Fig. 3(c) the anisotropies calculated using Eq. (1) from the results obtained with the two methods are displayed. Comparing the data sets, we find that the signal-to-noise ratio of new setup is about 4 times higher than that of the old setup. It should be noted that perfect cancellation of the IR intensity fluctuations is unfortunately not possible, since there is a 10% contribution to the fluctuations that occurs from shot to shot (this causes the initial drop from 1 to 0.9 in the autocorrelation function in Fig. 1). Decreasing these shot-to-shot fluctuations (by optimizing the IR source while monitoring the intensity autocorrelation function) should improve the signal-to-noise ratio of R even more. It should also be noted that since the phase retardation of the PEM varies slightly with the wavelength, the pump and probe polarizations are not perfectly parallel and perpendicular for IR frequencies far away from the frequency to which the PEM is adjusted. This effect can be corrected for by calibrating the setup using a sample with a time-independent, known anisotropy, e.g., a solid.

To conclude, the setup for polarization-resolved vibrational pump-probe measurements demonstrated here can improve the signal-to-noise ratio of anisotropy data significantly. This increase in accuracy is due to the photo-elastic modulator, which changes the probe pulse polarization of every other pulse by 90°. The parallel and perpendicular transient signals are then measured on a shot-to-shot basis, so that loss of accuracy caused by laser intensity fluctuations is prevented (provided the fluctuations occur on a time scale >2 ms). The improved signal-to-noise ratio allows a more accurate determination of the anisotropy at long delays, which often contain the most interesting information, but are difficult to measure. Finally, it may be noted that for a 10 kHz laser system, the method will work even better, since the IR intensity fluctuations of a 10-kHz laser system occur on the same time scale as those of a 1-kHz system [22].

References and Notes

1. C. P. Lawrence and J. L. Skinner, J. Chem. Phys. **118**, 264 (2003).
2. H. Graener, G. Seifert, and A. Laubereau, Chem. Phys. Lett. **172**, 435 (1990).
3. H. Graener and G. Seifert, J. Chem. Phys. **98**, 36 (1993).
4. R. Laenen and K. Simeonidis, Chem. Phys. Lett. **292**, 631 (1998).
5. A. J. Lock, S. Woutersen, and H. J. Bakker, J. Phys. Chem. A **105**, 1238 (2001).
6. K. J. Gaffney, P. H. Davis, I. R. Piletic, N. E. Levinger, and M. D. Fayer, J. Phys. Chem. A **106**, 12012 (2002).
7. K. Mazur, M. Bonn, and J. Hunger, J. Phys. Chem. B **119**, 1558 (2015).
8. D. Kraemer, M. L. Cowan, A. Paarmann, N. Huse, E. T. J. Nibbering, T. Elsaesser, and R. J. D. Miller, Proc. Natl. Acad. Sci. USA **105**, 437 (2008).
9. E. E. Fenn, D. B. Wong, and M. D. Fayer, Proc. Natl. Acad. Sci. USA **106**, 15243 (2009).
10. M. Ji, M. Odelius, and K. J. Gaffney, Science **328**, 1003 (2010).
11. K. J. Tielrooij, N. Garcia-Araez, M. Bonn, and H. J. Bakker, Science **328**, 1006 (2010).
12. M. Ji and K. J. Gaffney, J. Chem. Phys. **134**, 044516 (2011).
13. A. A. Bakulin and M. S. Pshenichnikov, Phys. Chem. Chem. Phys. **13**, 19355 (2011).
14. K. Ramasesha, S. T. Roberts, R. A. Nicodemus, A. Mandal, and A. Tokmakoff, J. Chem. Phys. **135**, 054509 (2011).
15. J. Hunger, K. J. Tielrooij, R. Buchner, M. Bonn, and H. J. Bakker, J. Phys. Chem. B **116**, 4783 (2012).
16. K. Ramasesha, L. De Marco, A. Mandal, and A. Tokmakoff, Nat. Chem. **5**, 935 (2013).
17. W. J. Smit and H. J. Bakker, J. Chem. Phys. **139**, 204504 (2013).
18. A. A. Bakulin, D. Cringus, P. A. Pieniazek, J. L. Skinner, T. L. C. Jansen, and M. S. Pshenichnikov, J. Phys. Chem. B **117**, 15545 (2013).
19. M. Panman, D. J. Shaw, B. Ensing, and S. Woutersen, Phys. Rev. Lett. **113**, 207801 (2014).
20. C. C. M. Groot and H. J. Bakker, J. Chem. Phys. **140**, 234503 (2014).
21. C.-S. Hsieh, R. K. Campen, A. C. V. Verde, P. Bolhuis, H.-K. Nienhuys, and M. Bonn, Phys. Rev. Lett. **107**, 116102 (2011).
22. P. Hamm (private communication, 2015).
23. M. Bonmarin and J. Helbing, Opt. Lett. **33**, 2086 (2008).
24. M. Bonmarin and J. Helbing, Chirality **21**, E298 (2009).
25. J. Helbing and M. Bonmarin, J. Chem. Phys. **131**, 174507 (2009).
26. M. Bonmarin and J. Helbing, Chimia **63**, 128 (2009).
27. In theory, this polarization dependence of the spectrograph transmittance should not pose any problems, since the absolute intensities of the pulses cancel out when constructing $\Delta A = -\log(T/T_0)$ from the intensities in the presence (T) and absence (T_0) of the pump pulse. However, the response of MCT-detector arrays is not perfectly linear, so that a large difference in the intensities of the parallel and perpendicular probe pulses can lead to systematic errors.
28. In the conventional setup, the pump and probe polarizations are at 45°, and $\Delta A_\parallel$ and $\Delta A_\perp$ are measured alternately during 600 ms to several seconds—the number depending on the pump-probe delay—by selecting the appropriate probe-polarization component using a polarizer placed on a computer-controlled rotation stage behind the sample.